

A SEARCH FOR EXOPLANETS AROUND NORTHERN CIRCUMPOLAR STARS. IV. SIX PLANET CANDIDATES TO THE K GIANTS, HD 44385, HD 97619, HD 106574, HD 118904, HD 164428, AND HD 202432

GWANGHUI JEONG,^{1,2} INWOO HAN,^{1,2} MYEONG-GU PARK,³ ARTIE P. HATZES,⁴ TAE-YANG BANG,³ SHENGHONG GU,^{5,6,7}
JINMING BAI,^{5,7} AND BYEONG-CHEOL LEE^{1,2}

¹*Korea Astronomy and Space Science Institute, 776, Daedeokdae-Ro, Yuseong-Gu, Daejeon 34055, Korea*

²*Korea University of Science and Technology, 217, Gajeong-ro Yuseong-gu, Daejeon 34113, Korea*

³*Department of Astronomy and Atmospheric Sciences, Kyungpook National University, Daegu 41566, Korea*

⁴*Thüringer Landessternwarte Tautenburg, Sternwarte 5, D-07778 Tautenburg, Germany*

⁵*Yunnan Observatories, Chinese Academy of Sciences, Kunming 650216, China*

⁶*University of Chinese Academy of Sciences, Beijing 100049, China*

⁷*Key Laboratory for the Structure and Evolution of Celestial Objects, Chinese Academy of Sciences, Kunming 650011, China*

(Received December 17, 2017; Revised xxxx xx, 2018; Accepted xxxx xx, 2018)

Submitted to ApJ

ABSTRACT

We report the discovery of long-period radial velocity (RV) variations in six intermediate mass K giant stars using precise RV measurements. These discoveries are part of the Search for Exoplanets around Northern Circumpolar Stars (SENS) survey being conducted at the Bohyunsan Optical Astronomy Observatory (BOAO). The nature of the RV variations was investigated by looking for photometric and line shape variations. We can find no variability with the RV period in these quantities and conclude that RV variations are most likely due to unseen sub-stellar companions. Orbital solutions for the six stars yield orbital periods in the range 418 – 1065 d and minimum masses in the range 1.9 – 8.5 M_J . These properties are typical on planets around intermediate mass stars. Our SENS survey so far has about an 8% confirmed planet occurrence rate, and it will provide better statistics on planets around giant stars when the survey is completed.

Keywords: planetary systems — stars: individual: HD 44385, HD 97619, HD 106574, HD 118904, HD 164428, and HD 202432 — techniques: radial velocities

1. INTRODUCTION

The measurement of stellar radial velocity (RV) is one of the most effective techniques employed in the search for exoplanets. At the Bohyansan Optical Astronomical Observatory (BOAO), we have been conducting an exoplanet search program around late-type giant stars since 2004. This program has made contributions to both exoplanet and asteroseismic studies around K giant stars (Han et al. 2008, 2010; Lee et al. 2011, 2012a,b, 2014a) and exoplanet detection around G giant stars (Omiya et al. 2009, 2012; Sato et al. 2013).

In 2010, we began a new program, the Search for Exoplanet around Northern circumpolar Stars (SENS; Lee et al. 2015). The main goal of SENS is to observe stars that are accessible year-round in order to have better sampling for our targets and thus increase the planet detection efficiency. The stars of SENS were selected from the *HIPPARCOS* catalog with visual magnitudes of $5.0 < m_v < 7.0$ and color indices of $0.6 < B - V < 1.6$. The original SENS sample consist of 224 stars – 5% dwarfs, 40% giant stars, and 55% unclassified stars. From SENS survey, we detected periodic RV variations around roughly twenty G, K, and M giant stars. Among them, HD 104985 (Sato et al. 2003), 11 Ursae Minoris (Döllinger et al. 2009), HD208527 & HD 220074 (Lee et al. 2013), HD 11755, HD 12648, HD 24064 and 8 Ursae Minoris (Lee et al. 2015), HD 36384, HD 52030, and HD 208742 (Lee et al. 2017) were later shown to host planetary companions.

In this paper, the observational strategy and data reduction are summarized in Section 2. Section 3 describes the stellar properties and analysis of each host stars. In Section 4, orbital solutions are described in detail. Some possible causes of the RV variations are examined in Section 5. The discussion about the results is presented in Section 6.

2. OBSERVATION

Observations were made with the high-resolution fiber-fed Bohyunsan Observatory Echelle Spectrograph (BOES; Kim et al. 2007) of the 1.8 m telescope at BOAO. An iodine (I_2) absorption cell is equipped in BOES for precise RV measurements. BOES has three fibers with 80 μm , 200 μm , and 300 μm of diameter, which give resolutions of $R = 90,000$, 45,000, and 27,000, respectively.

For our program, we used the 200 μm fiber. A typical exposure time of 20 minutes yielded a signal-to-noise ratio (S/N) of about 150. Since the start of the program in January 2010, we have collected 30 spectra each for HD 44385, HD 97619, HD 106574, HD 118904, HD 164428, and HD 202432. In order to check the in-

strumental stability, we have monitored an τ Ceti by standard since 2003. The long-term RV accuracy of BOES is $\sim 7.6 \text{ m s}^{-1}$.

The data reduction was performed with the IRAF package for bias subtraction, flat fielding, and order extraction, etc. Once we extracted the 1-D spectra from the raw data, precise RVs were measured using the program RVI2CELL (Han et al. 2007). Tables 3–?? list the measured RVs of each star.

3. STELLAR CHARACTERISTICS

We obtained the basic stellar parameters (the visual magnitude V , parallax π , spectral type, B-V, luminosity, and RV) of the stars from Anderson & Francis (2012) based on the *HIPPARCOS* catalog (ESA 1997). We also adopted more precise parallaxes from Gaia Collaboration et al. (2016). The effective temperature, $\log g$, metallicity ([Fe/H]), and microturbulent velocity (v_{micro}) were estimated from TGVIT (Takeda et al. 2005). For comparison, we also obtained the effective temperature from Ammons et al. (2006) and McDonald et al. (2012, 2017). We have estimated the projected rotational velocities using a line broadening technique (Takeda et al. 2008).

The stellar radii, masses, and ages were calculated using the online tool PARAM 1.3¹ (da Silva et al. 2006), which is based on a library of theoretical stellar isochrones (Girardi et al. 2000; Bressan et al. 2012) and Bayesian inference (Jørgensen & Lindegren 2005).

The stellar parameters of the observed stars are summarized in Table 1.

4. ORBITAL SOLUTIONS

Here we present the derived orbital parameters assuming that periodic RV variations are caused by Keplerian motion. An initial value of the period was determined using the Lomb-Scargle periodogram (L-S) analysis, which is appropriate for uneven sampled data and also gives an estimate of the false alarm probability (FAP) of the signal (Lomb 1976; Scargle 1982). Using this initial period, we estimated all the orbital elements by an iterated non-linear least-squares method. If a linear RV trend is shown, a slope is taken as an unknown parameter. Table 2 lists the orbital parameters for all stars.

4.1. HD 44385

The RV data of HD 44385 and the Keplerian motion are plotted in Fig. 1. The RVs cover more than five cycles and show a slight linear trend of $-6.9 \text{ m s}^{-1}\text{yr}^{-1}$,

¹ http://stev.oapd.inaf.it/cgi-bin/param_1.3/

Table 1. Stellar parameters for the stars.

Parameter	HD 44385	HD 97619	HD 106574	HD 118904	HD 164428	HD 202432	Ref.
Spectral type	K0	K0	K2 III	K2 III	K5	K2	1
m_v (mag)	6.771 ± 0.001	7.044 ± 0.001	5.883 ± 0.001	5.665 ± 0.001	6.388 ± 0.001	7.052 ± 0.001	1
$B - V$ (mag)	1.266 ± 0.007	1.315 ± 0.008	1.179 ± 0.005	1.219 ± 0.005	1.452 ± 0.008	1.206 ± 0.009	1
RV (km s ⁻¹)	-14.87 ± 0.20	-23.84 ± 0.17	-16.48 ± 0.29	13.72 ± 0.20	-8.16 ± 0.20	-2.23 ± 0.20	1
π (mas)	3.92 ± 0.41	4.93 ± 0.42	7.00 ± 0.28	7.93 ± 0.24	3.82 ± 0.29	6.40 ± 0.40	1
	4.68 ± 0.29	4.69 ± 0.33	–	9.02 ± 0.76	3.65 ± 0.27	6.20 ± 0.23	4
T_{eff} (K)	4499	4245	–	4511	4222	4569	2
	4326	4334	4482	4424	4257	4465	3
	4433 ± 125	4237 ± 125	4414 ± 125	4407 ± 125	4109 ± 125	4458 ± 125	5
	4440 ± 28	4355 ± 20	4501 ± 33	4469 ± 23	4119 ± 40	4549 ± 30	6
[Fe/H]	0.10 ± 0.07	-0.07 ± 0.07	-0.43 ± 0.04	-0.11 ± 0.09	-0.07 ± 0.10	0.16 ± 0.10	6
$\log g$ (cgs)	1.80	1.83	1.78	1.91	1.21	2.24	5
	2.00 ± 0.12	2.33 ± 0.09	2.18 ± 0.18	2.13 ± 0.10	1.62 ± 0.17	2.42 ± 0.12	6
v_{micro} (km s ⁻¹)	1.56 ± 0.13	1.54 ± 0.13	1.59 ± 0.06	1.39 ± 0.15	1.62 ± 0.16	1.32 ± 0.16	6
Age (Gyr)	1.8 ± 0.4	4.9 ± 1.7	4.6 ± 1.3	3.7 ± 1.6	2.7 ± 1.2	6.1 ± 2.6	6
R_* (R_\odot)	19.5	19.5	20.4	17.7	39.4	12.3	5
	18.2 ± 1.2	16.7 ± 1.3	17.1 ± 0.9	14.8 ± 1.3	35.4 ± 2.9	11.1 ± 0.3	6
M_* (M_\odot)	1.8 ± 0.2	1.3 ± 0.1	1.2 ± 0.1	1.4 ± 0.2	1.5 ± 0.2	1.2 ± 0.2	6
L_* (L_\odot)	233.2	122.8	152.2	152.4	469.3	63.9	1
	132.6 ± 11.1	109.8 ± 10.1	142.5 ± 9.8	105.6 ± 10.7	397.9 ± 37.8	54.0 ± 3.6	5
	116.0 ± 15.6	90.4 ± 14.2	108.1 ± 11.8	78.7 ± 13.9	325.0 ± 54.7	47.5 ± 2.9	6
$v_{\text{rot}} \sin i$ (km s ⁻¹)	2.6 ± 0.5	1.9 ± 0.5	1.7 ± 0.5	1.2 ± 0.5	2.8 ± 0.5	2.1 ± 0.5	6
$P_{\text{rot}} / \sin i$ (days)	354.1 ± 72.0	444.7 ± 122.0	508.9 ± 152.1	624.0 ± 265.7	629.6 ± 125.7	267.4 ± 64.1	6

References.— (1) Anderson & Francis (2012); (2) McDonald et al (2012); (3) Ammons et al (2006);
(4) Gaia Collaboration et al (2016); (5) McDonald et al (2017); (6) This work.

Table 2. Preliminary orbital solutions.

Parameter	HD 44385 b	HD 97619 b	HD 106574 b	HD 118904 b	HD 164428 b	HD 202432 b
P (days)	473.5 ± 4.9	665.9 ± 9.5	1065.7 ± 14.6	676.7 ± 19.1	599.6 ± 8.7	418.8 ± 2.9
K (m s ⁻¹)	104 ± 10	68 ± 6	149 ± 8	61 ± 8	109 ± 15	43 ± 3
$T_{\text{periastron}}$ (JD)	2455121 ± 37	2455238 ± 55	2455585 ± 360	2455478 ± 82	2455068 ± 46	2454908 ± 26
e	0.20 ± 0.20	0.23 ± 0.17	0.03 ± 0.03	0.31 ± 0.30	0.29 ± 0.22	0.21 ± 0.16
ω (deg)	292.18 ± 28.11	293.53 ± 23.97	44.66 ± 122.15	29.16 ± 31.02	203.11 ± 26.59	61.24 ± 21.76
$m \sin i$ (M_J)	5.9 ± 1.1	3.5 ± 1.3	8.5 ± 1.1	3.1 ± 1.2	5.7 ± 1.3	1.9 ± 0.4
a (AU)	1.4 ± 0.1	1.6 ± 0.1	2.2 ± 0.1	1.7 ± 0.1	1.6 ± 0.1	1.2 ± 0.1
Slope (m s ⁻¹ yr ⁻¹)	-6.9	11.5	2.4	1.0	1.2	4.4
N_{obs}	35	35	31	38	30	29
rms (m s ⁻¹)	41.5	26.2	44.0	33.2	51.6	12.4

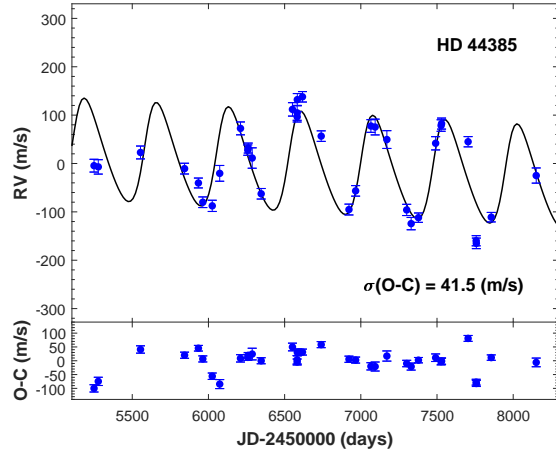


Figure 1. *Upper panel:* RVs of HD 44385 (blue dots) and a fitted Keplerian orbit (solid line). *Lower panel:* The residual RVs after subtracting the Keplerian fit.

such linear trend is also seen in the other five systems of this study. These linear RV variations may be caused by an unseen distant companion or due to some long-term and unknown intrinsic stellar variations. The orbit has a period, $P = 473.5 \pm 4.9$ days, an eccentricity, $e = 0.20 \pm 0.20$, and a semi-amplitude $K = 104 \pm 10$ m s⁻¹.

The RV residuals have an rms of 41.5 m s⁻¹, which is larger than the typical intrinsic RV variations of K giant stars. The scaling relationship of Kjeldsen & Bedding (1995) yields an amplitude of 15 m s⁻¹ for stellar oscillations, which may contribute to rms of the RV residuals. However, the excess residual RV scatter is still too large. We discuss these large residual RV scatter in Section 6.

4.2. HD 97619

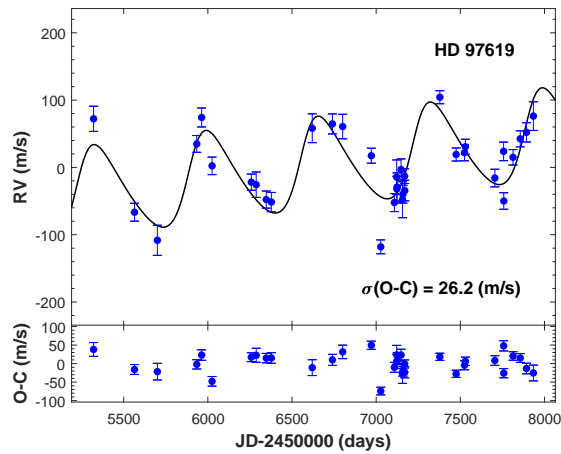


Figure 2. *Upper panel:* RVs of HD 97619 (blue dots) and a fitted Keplerian orbit (solid line). *Lower panel:* The residual RVs after subtracting the Keplerian fit.

The RV data of HD 97619 and the Keplerian orbit are plotted in Fig. 2. The RVs cover more than three cycles and these also show a slight linear trend of 11.5 m s⁻¹yr⁻¹, again possibly due a third body in the system. The best Keplerian fit yields the orbital elements of $P = 665.9 \pm 9.5$ days, $e = 0.23 \pm 0.17$, and $K = 68 \pm 6$ m s⁻¹. The host star has a mass just a little higher than the Sun, as the other host star HD 202432. It hosts a planet candidate with the lowest mass among the companions in the present study. The rms of RV residuals is 26.2 m s⁻¹ consistent with the expected RV scatter (so called “jitter”).

4.3. HD 106574

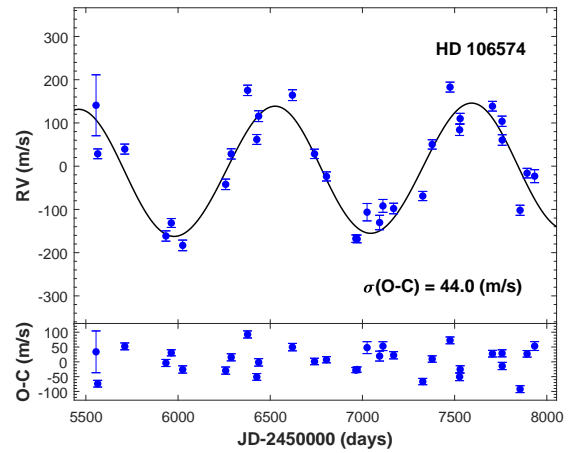


Figure 3. *Upper panel:* RVs of HD 106574 (blue dots) and a fitted Keplerian orbit (solid line). *Lower panel:* The residual RVs after subtracting the Keplerian fit.

The RV data of HD 106574 and the best Keplerian orbital fit are plotted in Fig. 3. The RVs cover about two cycles. The orbit has a period of 1065.7 ± 14.6 days, an eccentricity of 0.03 ± 0.03 , and a semi-amplitude of 149 ± 8 m s⁻¹. Unlike other five systems, this system has a nearly circular orbit. The planet candidate is the most massive among our six stars. The residuals have an rms of 44.0 m s⁻¹. This is considerably larger than the value of 21 m s⁻¹ predicted by the Kjeldsen & Bedding (1995) relationship. This possibly indicates an additional source of stellar variability as HD 44385.

4.4. HD 118904

The RV data of HD 118904 and the best Keplerian orbital fit are plotted in Fig. 4. The RVs cover more than three cycles. The orbital fit yields a period of 676.7 ± 19.1 days, an eccentricity of 0.31 ± 0.30 , and a semi-amplitude of 61 ± 8 m s⁻¹. The rms RV residuals have a value of 33.2 m s⁻¹, also the normal case for a K giant star.

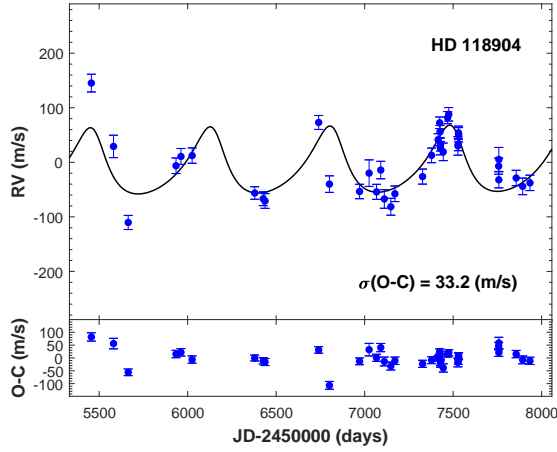


Figure 4. *Upper panel:* RVs of HD 118904 (blue dots) and a fitted Keplerian orbit (solid line). *Lower panel:* The residual RVs after subtracting the Keplerian fit.

4.5. HD 164428

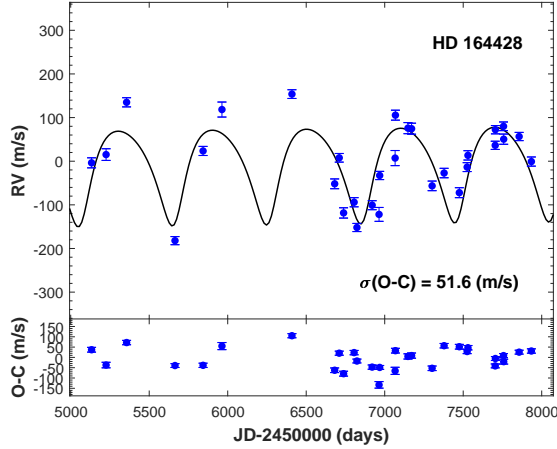


Figure 5. *Upper panel:* RVs of HD 164428 (blue dots) and a fitted Keplerian orbit (solid line). *Lower panel:* The residual RVs after subtracting the Keplerian fit.

The RV data of HD 164428 and the Keplerian orbital fit are plotted in Fig. 5. The RVs cover more than four cycles. The orbit has a period of 599.6 ± 8.7 days, an eccentricity of 0.29 ± 0.22 , and a semi-amplitude of 109 ± 15 m s⁻¹. The planet candidate has a similar mass as HD 44385 b. The rms scatter about the orbit is 51.6 m s⁻¹, which is the largest jitter seen in our six systems, and is consistent with the predicted value of ~ 50 m s⁻¹ for the stellar oscillations according to scaling relationships.

4.6. HD 202432

The RV data of HD 202432 and the best Keplerian orbital fit are plotted in Fig. 6. The RVs cover six cycles and show a slight linear trend of 4.4 m s⁻¹yr⁻¹. The

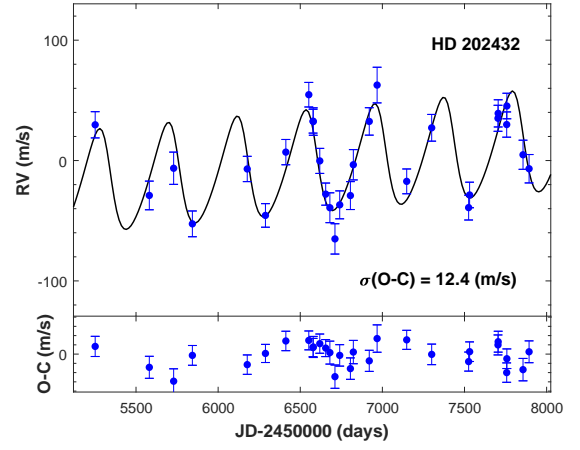


Figure 6. *Upper panel:* RVs of HD 202432 (blue dots) and a fitted Keplerian orbit (solid line). *Lower panel:* The residual RVs after subtracting the Keplerian fit.

Keplerian fit yields a period of 418.8 ± 2.9 days, an eccentricity of 0.21 ± 0.16 , and a semi-amplitude of 43 ± 3 m s⁻¹. An rms of RV residuals is 12.4 m s⁻¹, a value consistent with the expected velocity amplitude of 10 m s⁻¹ for stellar oscillations.

The RV measurements phased using best-fit orbital periods for all six stars is shown in Figure 7. All planet candidates except HD 106574 b have a relatively high eccentricity. However, we have a relatively small number of observations and these stars show significant intrinsic variability. The coarse sampling plus large scatter may result in an artificially high eccentricity. More data are needed to resolve this.

5. THE CAUSE OF THE RV VARIATIONS

The periodic variations of RVs may be also intrinsic to the star such as rotational modulation or stellar pulsations by surface features. To identify the nature of the RV variations, we investigated Ca II H lines, photometric data, and spectral line profile variations.

5.1. Surface activity

A rotating star with surface features such as spots or plage caused by magnetic activity will exhibit periodic RV variations, which can be misinterpreted as a planetary signal (Queloz et al. 2001). The Ca II H line (3968.5 Å) has often been used as a good indicator of stellar activity (Eberhard & Schwarzschild 1913). If there is a chromospheric activity, an emission line may appear at the center of Ca II H absorption line profile on the core of the line may be partially filled in.

The Ca II H lines of each host star are shown in Fig. 8. There appears to be no noteworthy emission in the core of the Ca II H line for any target stars.

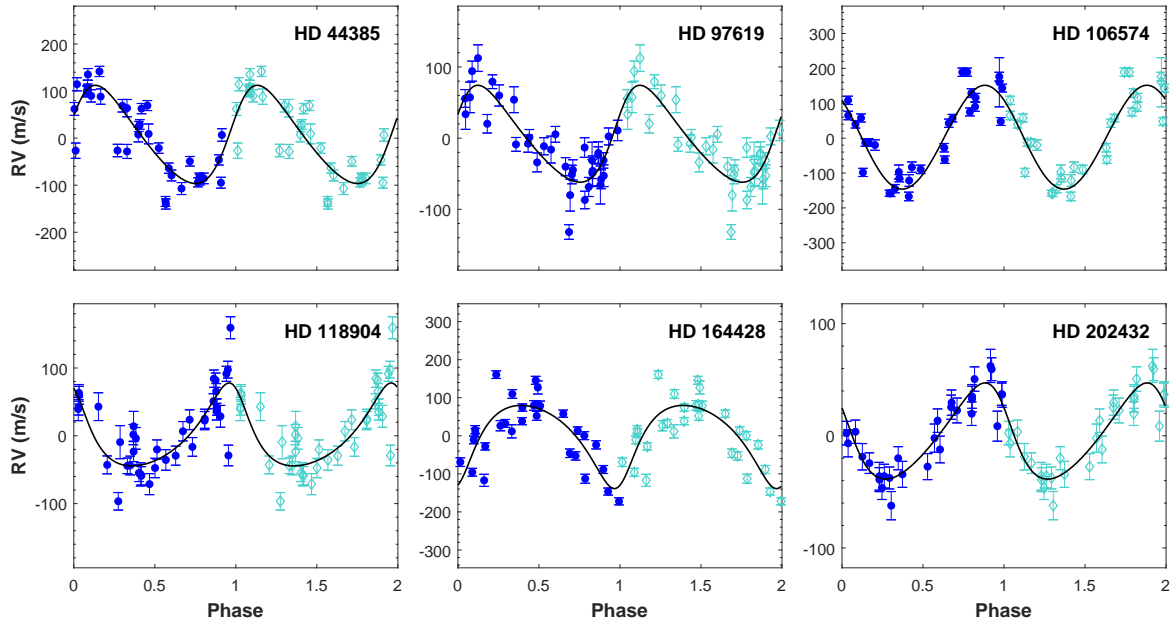


Figure 7. The phase folded RV curves of all stars

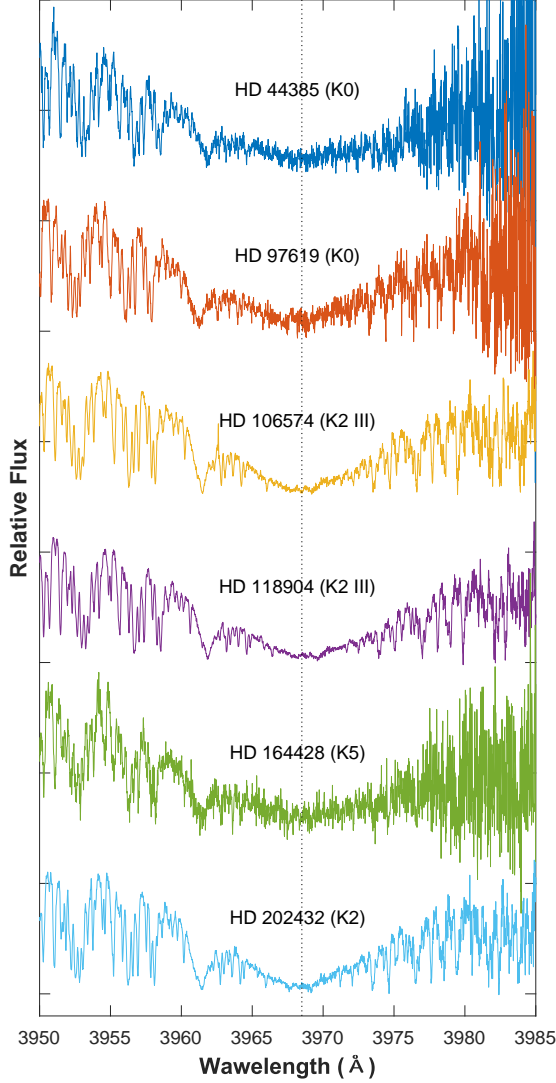


Figure 8. Spectra in the region of the Ca II H line. The vertical dotted-line is located in the core of the Ca II H profiles (3968.5 Å).

5.2. Photometric variations

To check for any photometric variations of the stars, we used *HIPPARCOS* archival data. *HIPPARCOS* data cover the period between November 1989 and March 1993. Although the measurements are not contemporaneous with our observations, it is still useful to check whether the *HIPPARCOS* data show any periodic photometric variability. The *HIPPARCOS* catalogue provides a total of 160, 148, 143, 119, 122, and 114 observations of the HD 44385, HD 97619, HD 106574, HD 118904, HD 164428, and HD 202432, respectively.

The rms scatter of the data is 0.011, 0.011, 0.007, 0.011, 0.009, and 0.010 mag for each star, respectively. Their scatter is comparable to the photometric uncertainties of *HIPPARCOS* data which ranges from 0.007

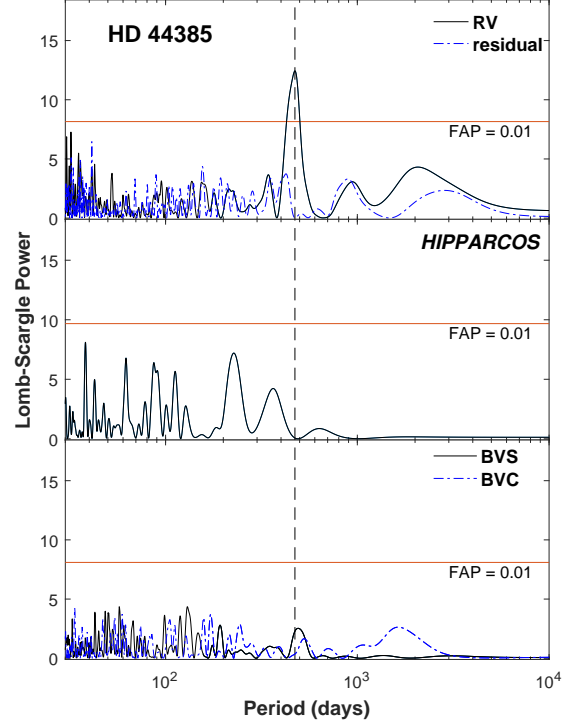


Figure 9. Top to bottom: L-S periodogram of the RV measurements, residual RVs, *HIPPARCOS* photometry, and the line bisectors of the span and curvature for HD 44385. The vertical dashed line represents 473 d period.

to 0.011 mag. We do not see any significant photometric variability of the stars. We also checked periodicity of *HIPPARCOS* data from the L-S periodogram, and could not find any significant periodicity corresponding to that of the RV variations (middle panels in the Figs. 9–14).

5.3. Line bisector variations

The examination of spectral line shape is an important tool to help identify other origins of RV variations than Keplerian motion (Hatzes & Cochran 1998). Orbital motion by a companion should cause a Doppler shift without a change of the line shape, whereas RV variations caused by rotational modulation from stellar surface structure should be accompanied by line shape variations. We thus investigated the change of the spectral line shapes using two indicators: The bisector velocity curvature (BVC) and the bisector velocity span (BVS).

To measure the line bisectors, we selected the lines Ca I 6122.2, 6439.1, 6462.6, 6717.7; Cr I 6330.1; Fe I 6141.7, 6393.6, 6411.7, 6677.9, 6750.2; Fe II 6151.6; Ni I 6643.6, 6767.8; Ti I 6085.2, 6742.6; V I 6039.7, 6081.4. These lines are free from I₂ and telluric absorption lines and are relatively deep. The L-S periodogram of bisectors do not show any significant periodicity associ-

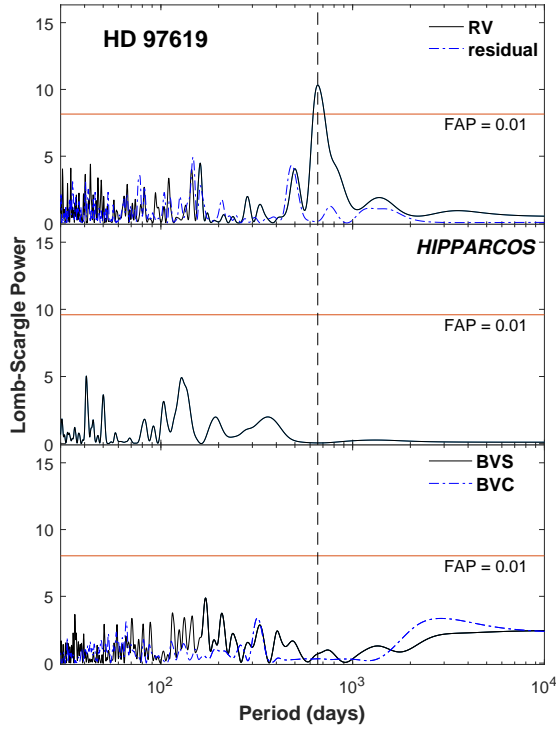


Figure 10. Top to bottom: L-S periodogram of the RV measurements, residual RVs, *HIPPARCOS* photometry, and the line bisectors of the span and curvature for HD 97619. The vertical dashed line represents 667 d period.

ated with those of RV variations (bottom panels in the Figs 9–14).

6. DISCUSSION

We have found long-period RV variations of six K-giant stars. The stars show no variations in the line shapes as measured by the spectral line bisectors. HD 44385 does show a weak signal in the bisector curvature measurements (BVS), but this does not seem to be significant ($\text{FAP} \geq 0.1$). We note that a lack of bisector measurements is not proof of the planetary nature. High quality bisector measurements are difficult to make as these require high spectral resolution and high S/N data. In general these are of much lower quality than the RV measurements. If we found bisector variations with the RV period, then the planet hypothesis is refuted. On the other hand, a lack of bisector variations is not sufficient proof of the existence of the planet. It could well be that a phenomenon produces measurable RV variations, but small bisector variations that are difficult to measure.

The stars also seem to show a lack of variations in the *HIPPARCOS* photometry. Only one star, HD 106574, shows a weak peak in the L-S periodogram at the RV period. Again, this peak seems to be of low significance.

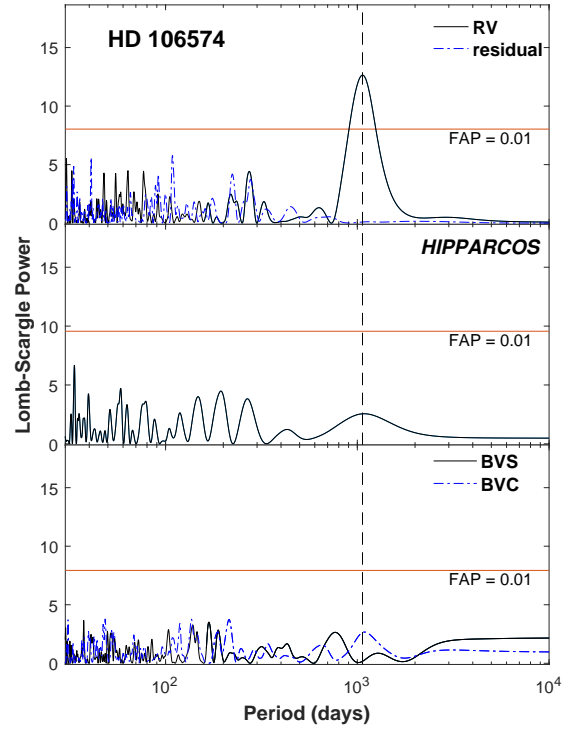


Figure 11. Top to bottom: L-S periodogram of the RV measurements, residual RVs, *HIPPARCOS* photometry, and the line bisectors of the span and curvature for HD 106574. The vertical dashed line represents 1071 d period.

However, the lack of photometric variations is only suggestive as the *HIPPARCOS* measurements were not contemporaneous to our data.

HD 44385, HD 106574, and HD 118904 have larger RV scatters than those predicted by the [Kjeldsen & Bedding \(1995\)](#) relationship. Later spectral type stars, such as HD 106574 and HD 118904, show larger RV scatters than those given in [Sato et al. \(2005\)](#); [Hekker et al. \(2006\)](#). [Lee et al. \(2012b\)](#) also have detected an exoplanet with similar orbital parameters and rms of the RV residuals. Some more exoplanets discovered using BOES have shown large RV scatters ([Lee et al. 2013, 2014a,b, 2015](#); [Hatzes et al. 2015, 2018](#)).

RV scatter in giant stars may have its origin not only from the stellar pulsations but also from the stellar activities. [Hatzes & Cochran \(1993\)](#) found RV variations in α Boo with a period of 233 d and an amplitude of $\sim 200 \text{ m s}^{-1}$. This RV period was the same period found in the He I 10830 variations in this star by [Lambert \(1987\)](#). He I 10830 is a chromospheric activity indicator. In this case, large RV variations are clearly due to the stellar activity.

Activity in giant stars is poorly understood and it may be that these are often not accompanied by variations in the “classic” indicators of stellar activity. We do not

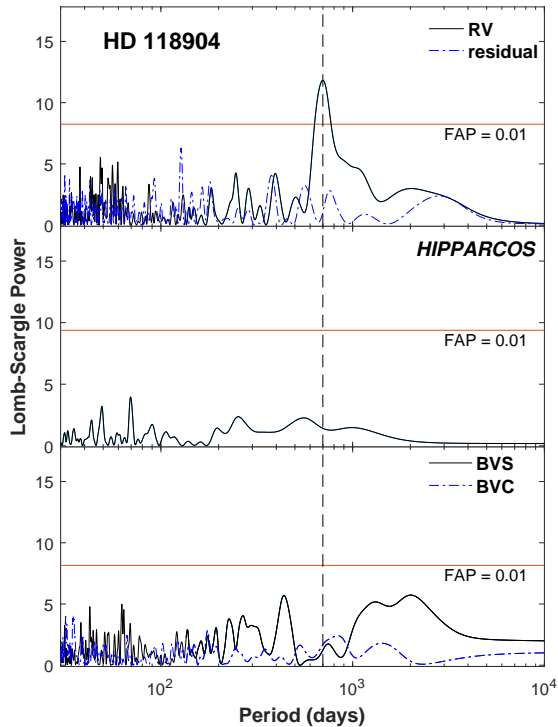


Figure 12. *Top to bottom:* L-S periodogram of the RV measurements, residual RVs, *HIPPARCOS* photometry, and the line bisectors of the span and curvature for HD 118904. The vertical dashed line represents 675 d period.

know the timescales or RV amplitudes of such activity jitter for these stars, which may have contributed to the RV scatters seen in some of our stars. The exact cause of large RV scatters seen in our stars is yet to be understood by further study.

Rotating stars with surface features can also exhibit periodic RV variations which can be mimic a “planetary like” signal. Our stars appear to be relatively inactive as shown by an absence of emission in the core of Ca II H lines. Another check on rotational modulation can come from estimates of the rotational period of the star.

From $v_{\text{rot}} \sin i$ and R_* (Table 1) we estimate upper limits on the rotational period of 354.1 ± 72.0 days for HD 44385, 444.7 ± 122.0 days for HD 97619, 508.9 ± 152.1 days for HD 106574, 624.0 ± 265.7 days for HD 118904, 629.6 ± 125.7 days for HD 164428, and 267.4 ± 64.1 days for HD 202432. HD 118904 and HD 164428 have estimated rotation periods comparable to the RV periods. In the case of HD 44385, HD 97619, HD 106574 and HD 202432 are the maximum rotational periods significantly larger than the RV periods. For these four stars our estimated rotational periods provide further support that we are not seeing rotational modulation.

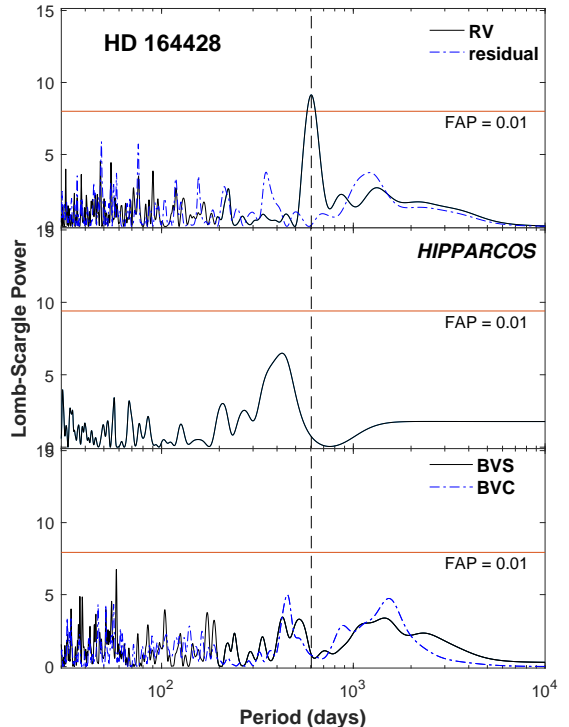


Figure 13. *Top to bottom:* L-S periodogram of the RV measurements, residual RVs, *HIPPARCOS* photometry, and the line bisectors of the span and curvature for HD 164428. The vertical dashed line represents 594 d period.

Another explanation for the RV variations in the six stars is a new, unknown form of stellar oscillations. One possibility is oscillatory convective modes. These have been proposed to explain the long-period variables (Saio et al. 2015), stars that are more evolved than the K giant stars of our work. Coincidentally, only one of stars, HD 164428, is rather evolved with stellar radius larger than $20 R_{\odot}$. However, given that we know so little about long-period oscillations in K giant stars it seems that at the present time the most likely explanation for the RV variations in our stars is Keplerian motion by planetary companions.

All of our targets are evolved intermediate mass stars. If the variations are due to planetary companions our detections add to the sample of exoplanets around stars more massive than the sun. Two of our stars have masses $\geq 1.5 M_{\odot}$. Of the approximately 2200 exoplanets with good orbits and planet mass determinations, less than 5% of the host stars have masses greater than $1.5 M_{\odot}$ (source: exoplanets.org). Exoplanets around host stars with $M \geq 2 M_{\odot}$ have a median $m \sin i$ of $2.7 M_J$ and a median orbital period of ~ 400 d. Thus the companions to our six K giants have properties that are typical for planets around massive stars: massive giant

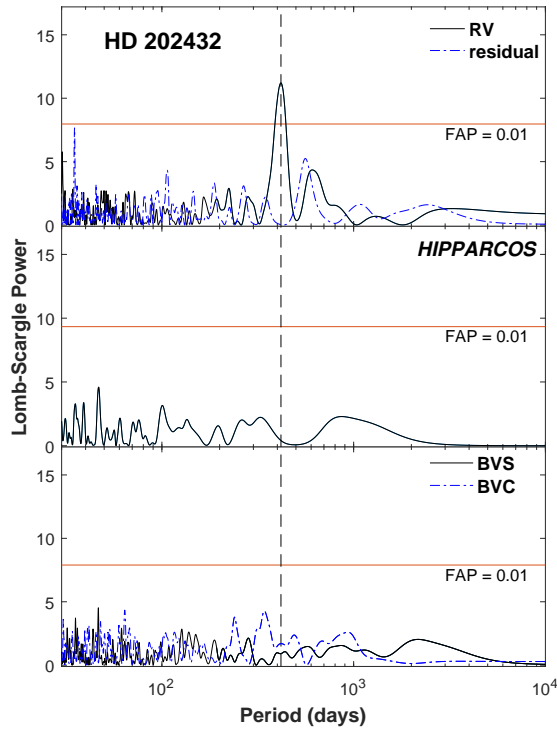


Figure 14. *Top to bottom:* L-S periodogram of the RV measurements, residual RVs, *HIPPARCOS* photometry, and the line bisectors of the span and curvature for HD 202432. The vertical dashed line represents 422 d period.

planets ($1.9 - 8.5 M_J$) with orbital periods of several hundreds of days.

Although the SENS survey is not yet complete, at this stage we can still make a rough estimate of the planet frequency of our sample. We have found periodic variations in 31 of our sample of 224 stars. Among these, 17 stars have confirmed planets which is a planet occurrence rate of about 8%. If all the RV variations are planetary in nature, then the occurrence rate can be as high as $\approx 15\%$. This is largely in line with the expectation that $\sim 10\%$ giant stars have planetary companions (Mulders et al. 2015). A more detailed analysis of the statistics can be made once the SENS survey is completed.

This work is supported by the KASI (Korea Astronomy and Space Science Institute) through grant No. 2017-1-860-01. BCL acknowledges partial support by the KASI grant 2017-1-830-03. Support for MGP and TYB was provided by the KASI under the R&D program supervised by the Ministry of Science, ICT and Future Planning and by the National Research Foundation of Korea to the Center for Galaxy Evolution Research (No.2017R1A5A1070354). TYB was also supported by BK21 Plus of National Research Foundation of Korea. S.G. would like to thank NSFC for the financial support through the grant No. U1531121. This research made use of the SIMBAD database, operated at the CDS, Strasbourg, France. We thank BOAO for its generous support.

REFERENCES

- Ammons, S. M., Robinson, S. E., Strader, J., Laughlin, G., Fischer, D., & Wolf, A. 2006, *ApJ*, 638, 1004
- Anderson, E., & Francis, C. 2012, *Astronomy Letters*, 38, 331
- Bressan, A., Marigo, P., Girardi, L., Salasnich, B., Dal Cero, C., Rubele, S., & Nanni, A. 2012, *MNRAS*, 427, 127
- da Silva, L., et al. 2006, *A&A*, 458, 609
- Döllinger, M. P., Hatzes, A. P., Pasquini, L., Guenther, E. W., & Hartmann, M. 2009, *A&A*, 505, 1311
- Eberhard, G., & Schwarzschild, K. 1913, *ApJ*, 38, 292
- ESA. 1997, *VizieR Online Data Catalog*, 1239, 0
- Gaia Collaboration, et al. 2016, *A&A*, 595, A1
- Girardi, L., Bressan, A., Bertelli, G., & Chiosi, C. 2000, *A&AS*, 141, 371
- Han, I., Kim, K.-M., Byeong-Cheol, L., & Valyavin, G. 2007, *Publication of Korean Astronomical Society*, 22, 75
- Han, I., Lee, B.-C., Kim, K.-M., & Mkrtichian, D. E. 2008, *Journal of Korean Astronomical Society*, 41, 59
- Han, I., Lee, B. C., Kim, K. M., Mkrtichian, D. E., Hatzes, A. P., & Valyavin, G. 2010, *A&A*, 509, A24
- Hatzes, A. P., & Cochran, W. D. 1993, *ApJ*, 413, 339
- Hatzes, A. P., & Cochran, W. D. 1998, in *Astronomical Society of the Pacific Conference Series*, Vol. 154, *Cool Stars, Stellar Systems, and the Sun*, ed. R. A. Donahue & J. A. Bookbinder, 311
- Hatzes, A. P., et al. 2015, *A&A*, 580, A31
- Hatzes, A. P., et al. 2018, *AJ*, 155, 120
- Hekker, S., Reffert, S., Quirrenbach, A., Mitchell, D. S., Fischer, D. A., Marcy, G. W., & Butler, R. P. 2006, *A&A*, 454, 943
- Jørgensen, B. R., & Lindegren, L. 2005, *A&A*, 436, 127
- Kim, K.-M., et al. 2007, *PASP*, 119, 1052
- Kjeldsen, H., & Bedding, T. R. 1995, *A&A*, 293, 87
- Lambert, D. L. 1987, *ApJS*, 65, 255

- Lee, B.-C., Han, I., & Park, M.-G. 2013, *A&A*, 549, A2
- Lee, B.-C., Han, I., Park, M.-G., Mkrtichian, D. E., Hatzes, A. P., & Kim, K.-M. 2014a, *A&A*, 566, A67
- Lee, B.-C., Han, I., Park, M.-G., Mkrtichian, D. E., Jeong, G., Kim, K.-M., & Valyavin, G. 2014b, *Journal of Korean Astronomical Society*, 47, 69
- Lee, B.-C., Han, I., Park, M.-G., Mkrtichian, D. E., & Kim, K.-M. 2012a, *A&A*, 546, A5
- Lee, B.-C., et al. 2017, *ApJ*, 844, 36
- Lee, B.-C., Mkrtichian, D. E., Han, I., Kim, K.-M., & Park, M.-G. 2011, *A&A*, 529, A134
- Lee, B.-C., Mkrtichian, D. E., Han, I., Park, M.-G., & Kim, K.-M. 2012b, *A&A*, 548, A118
- Lee, B.-C., et al. 2015, *A&A*, 584, A79
- Lomb, N. R. 1976, *Ap&SS*, 39, 447
- McDonald, I., Zijlstra, A. A., & Boyer, M. L. 2012, *MNRAS*, 427, 343
- McDonald, I., Zijlstra, A. A., & Watson, R. A. 2017, *MNRAS*, 471, 770
- Mulders, G. D., Pascucci, I., & Apai, D. 2015, *ApJ*, 798, 112
- Omiya, M., et al. 2012, *PASJ*, 64, 34
- Omiya, M., et al. 2009, *PASJ*, 61, 825
- Queloz, D., et al. 2001, *A&A*, 379, 279
- Saio, H., Wood, P. R., Takayama, M., & Ita, Y. 2015, *MNRAS*, 452, 3863
- Sato, B., et al. 2003, *ApJL*, 597, L157
- Sato, B., Kambe, E., Takeda, Y., Izumiura, H., Masuda, S., & Ando, H. 2005, *PASJ*, 57, 97
- Sato, B., et al. 2013, *PASJ*, 65, 85
- Scargle, J. D. 1982, *ApJ*, 263, 835
- Takeda, Y., Ohkubo, M., Sato, B., Kambe, E., & Sadakane, K. 2005, *PASJ*, 57, 27
- Takeda, Y., Sato, B., & Murata, D. 2008, *PASJ*, 60, 781

Table 3. RV measurements for HD 44385. Table 3 is published in its entirety in the electronic edition of the *Astronomical Journal*. It includes all six stars. Only HD 44385 is shown here for guidance regarding its form and content.

JD -2450000	ΔRV m s^{-1}	$\pm\sigma$ m s^{-1}	JD -2450000	ΔRV m s^{-1}	$\pm\sigma$ m s^{-1}
5249.186772	-4.5	13.2	6739.992829	56.6	10.9
5277.062617	-7.0	14.9	6922.262909	-95.2	11.2
5554.202620	22.8	13.3	6965.959830	-56.6	10.9
5843.317817	-10.6	11.1	7066.218427	77.5	13.1
5934.119026	-40.3	10.2	7094.061052	75.4	16.3
5963.063139	-80.1	11.0	7171.018942	49.5	18.4
6024.980916	-87.6	11.6	7301.155470	-96.0	11.6
6074.004223	-20.4	16.3	7330.319704	-124.3	12.7
6210.342839	72.6	13.3	7378.167893	-112.0	9.7
6258.199914	27.7	10.7	7491.026213	41.8	13.7
6261.229862	31.9	10.3	7526.987711	78.5	11.9
6287.184819	11.3	21.1	7529.996251	82.5	11.4
6346.097590	-62.6	10.9	7704.047239	45.0	10.6
6551.347025	111.9	13.9	7757.136001	-159.7	10.5
6582.281632	104.7	15.4	7758.104706	-165.1	10.9
6582.296436	96.6	10.8	7856.004581	-111.0	9.8
6583.251127	132.0	12.6	8151.089358	-24.9	15.7
6617.049357	137.9	10.8			